The Version of Record published in the International Journal of Advanced Manufacturing Technology, vol. 122, nº 9-10. 2022. pp. 3969-3981 is available online at: https://doi.org/10.1007/s00170-022-10150-1

Effect of Graphene Additive on Cutting Forces and Temperature during the Trimming Process of CFRP

Ronan Mathieu[1], Mohamed Ali Charfi[1], Jean-Francois Chatelain*[1], Claudiane Ouellet-Plamondon[1], Roger Serra[2], Gilbert Lebrun[3]

[1] École de Technologie Supérieure, 1100 Notre Dame West, QC H3C 1K3
Jean-francois.chatelain@etsmtl.ca

[2] INSA Centre Val de Loire, 3 Rue de la Chocolaterie, 41000 Blois, France

[3] Université du Québec à Trois-Rivières, 3351 Boulevard des Forges, QC G8Z 4M3

Abstract: Carbon Fiber Reinforced Polymer (CFRP) composite materials are massively used since the last decades in many contemporary applications, especially in aerospace for their strength to density and stiffness to density ratios which are higher than alloys. On the other hand, CFRP are known to be difficult to machine compared to metals due to their heterogeneous and anisotropic structure. Common damages like delamination, fiber loosening and pull out, uncut fibers as well as mechanical and thermal damages to the epoxy matrix are observed after machining. This research studies the effect of graphene particles addition in epoxy matrix of CFRP on the cutting temperature, in a global objective of improving the machinability and cutting tool life. Thereby, four modified resin plates (0 %wt, 0,25 %wt, 3 %wt and 10 %wt of graphene) without carbon fibers (nanocomposite plates only) were first molded. Next, three CFRP laminates with different percentages of graphene (0 %wt 0,25 %wt and 3 %wt) were manufactured using a combination of vacuum bagging and hydraulic pressing in order to guarantee a good fillers' distribution within the composite plates and a consistent fiber volume fraction. The trimming experiments were performed using a Polycrystalline Diamond (PCD) tool which was selected for its well-known machining performance. As expected, the tool wear was nonexistent on nanocomposites. For CFRP plates, the tool wear remained in its break-in zone throughout the experiment (final Vb $\approx 0{,}051 \ll 0{,}3\ mm$ for a final length cut of 4,5 m). The cutting tool's temperature increases with graphene concentration for both nanocomposites and CFRP samples. However, the temperature increase of CFRP plates was reduced by 30%

with a graphene concentration of 3 %wt. The feed forces were also greatly reduced (up to 43%) with graphene when machining CFRP.

Keywords: CFRP, composite, graphene, machining, temperature, cutting forces

The Version of Record published in the International Journal of Advanced Manufacturing Technology, vol. 122, nº 9-10. 2022. pp. 3969-3981 is available online at: https://doi.org/10.1007/s00170-022-10150-1

1 Introduction

The industrial use of composite materials, more specifically fibre-reinforced polymer composites (FRPC), is impinged by the lack of knowledge related to machining. It is a well-known fact that composites are more and more used for their highly specific mechanical properties [1]. In the aeronautical field, the last generation of airliners, Airbus 350 XWB and Boeing 787, are composed by more than 50 % of carbon fibre-reinforced polymer (CFRP) [2]. Precise manufacturing processes are used to produce near net shape parts but machining operations like drilling, trimming or surface milling still are required to comply to dimensional and geometrical specifications. The machinability of CFRP has been the subject of many research over the last decade. As opposed to metals, common damages like delamination, fibers pull out, uncut fibers as well as mechanical and thermal damages to the epoxy matrix are observed when machining FRP materials [3]. The issue related to such damages is important since they have been found to alter the mechanical properties of the material [9]. Machining is a complex process which relates different factors such as the cutting tool type (shape, material), the material type (constituents, processing, mechanical and physical characteristics) and the cutting parameters. The machinability of composites has been found to greatly depends on the properties of each constituent and on their fiber content [4]. Fibers are considered to have the main impact on the resulting quality of machined components and the cutting tool wear [4,6]. The tools wear out prematurely because of the anisotropic and non-homogeneous nature of composites as well as the abrasiveness of the reinforcements [6]. In addition, the machining operations are usually performed without lubrication (dry machining) since these materials

may be sensitive to moisture. In fact, using cutting fluid has been found to cause delamination and cracks which irrevocably deteriorate the material properties [7,8].

Polymer matrices have very poor thermal conductivity. As a result, the heat generated during the cutting process is difficult to extract, as opposed to metallic material, and thus will concentrate on a small cut area and within the cutting tool [9]. As a consequence, the mechanical properties of the machined component may be irrevocably impacted by thermal and mechanical damages, especially if the cutting temperature exceeds the glass transition temperature (Tg) of the matrix [10,11].

Tool wear plays a very important role on the surface condition of machined parts, but also on the deterioration of the matrix [12]. The machining of composite materials sorely test cutting tools which wear out quickly due to their anisotropic nature. In addition, these materials are very poor thermal conductors, so high temperatures in the cutting area are observed. Moreover, tool wear increases drastically above a critical temperature [13].

Graphene is a recent material which has very high thermal and electrical conductivity with a large specific surface area [14]. This large specific surface combined with Van der Waals interactions make exfoliation difficult when mixed to a polymeric material. The graphene particles tend to re-agglomerate naturally due to the strong Van der Waals force when mixed in polymer (like epoxy in this study), which explains drastic decrease in performance due to stress concentration. Conversely, a good exfoliation distributes stress and improves the mechanical properties of the material [15,16]. Consequently, when more individual particles are in contact with the polymer, the higher the probability of interactions between the particles and polymer, and more efficient is the stress transfer [17]. Well-exfoliated graphene into an organic matrix leads to the development of nanocomposites with interesting properties. Mechanical performance, thermal and electrical conductivity are significantly increased [18]. Small concentrations of graphene within the epoxy considerably improve the physical and chemical properties of the resin [15]. Thermal conductivity is increased thanks to the large specific surface area of graphene. This also depends on the dispersion, the interaction with the resin, but also the

orientation of nanoparticles. Thermal conductivity tends to increase linearly with graphene [19]. In CFRP, a covalent interaction can take place between graphene, carbon fibers and the resin, which improves the mechanical properties. Thermal and electrical properties are at the time improved [20].

Very few studies have looked at adding fillers to the matrix of CFRP. Nonetheless, the interests of graphene during the machining of GFRP has been demonstrated, especially with a drop in cutting temperatures [21]. The aim of this research is to study the effect of adding graphene particles (for their thermal properties) in CFRP and epoxy matrix on the cutting temperature. At the same time, their mechanical properties have to be at least maintained or increased. This study is a part of a global objective of improving the CFRP machinability and reduce cutting tool wear. Indeed, enhancing the tool life is a major issue when considering the economics of the overall machining process of high-performance composite components. Thus, two manufacturing processes have been studied to guarantee a homogeneous graphene distribution as well as consistent CFRP and nanocomposite plates. We also investigated the cutting and plate temperature thanks to thermocouples fixed to PCD cutting tools and to an infrared imaging thermal camera.

2 Methodology

Two types of composite materials have been manufactured: CFRP with 90° fibers (the most severe case [21,5]) which reflect an industrial reality, and nanocomposites (without fibers) which allow the study of graphene without tool wear. A total of seven different laminates were made, three for CFRP and four for nanocomposites. The CFRP plates have three different concentrations: 0 (reference concentration), 0.25 (best mechanical performances according to [23]) and 3 %wt (maximum concentration allowing the manufacturing of plates). Regarding the nanocomposite's plates, the first three concentrations (0, 0.25, 3 %wt) of nanoparticles are the same as for CFRP plates to allow comparison in temperature variation trends. The fourth plate represents a borderline case not feasible with CFRP with

a high concentration of graphene, 10% wt. Table 1 summarizes the graphene concentrations in the molded plates. The final dimensions of CFRP and nanocomposite laminates are 30×30 centimetres.

Table 1:Experimental plan

	Nanocomposite				**CFRP**		
Graphene concentration (%wt)	0	0.25	3	10	0	0.25	3
Plate numbering	1	2	3	4	I	II	III

2.1 Manufacturing process

All plates (CFRP and nanocomposite) were produced using epoxy resin (Marine 820 from Axson Technologies) with graphene (GrapheneBlack 0X) supplied by NanoXplore which has already proved a thermal interest with thermoplastic [19]. To calculate the amount of graphene required from the mass of neat epoxy, the following equations 1 and 2 were considered.

$$M_t = M_r + M_h + M_g \text{ with } \begin{cases} M_h = 0{,}18 \cdot M_r \ \ (data\ sheet) \\ M_g = \%_{wt,g} \cdot M_t \end{cases} \quad (1)$$

Then,

$$M_g = \frac{1{,}18 \cdot M_r \cdot \%_{wt,g}}{1 - \%_{wt,g}} \quad (2)$$

M_t is the total weight (g); M_r is the resin weight (g); M_h is the hardener weight (g); M_g is the graphene weight (g); $\%_{wt,g}$ is the graphene weight percentage (Ø).

In order to homogenize the resin with the graphene particles, we used a high-speed shearing mixer (Silverson L5M-A) with five different speeds and duration (Table 2): 1000 (2 min, 1 time), 3500 (2 min, 1 time), 6000 (2 min, 1 time), 8000 (2 min, 1 time), and 10000 RPM (2 min, 3 times). These parameters were selected through experiments to avoid overheating of the resin and prevent agglomeration of the graphene.

Table 2 Shear mixing step

# Times	Duration (min)	Speed (RPM)
1	2	1 000
1	2	3 500
1	2	6 000
1	2	8 000
3	2	10 000

The mixing took place in a bath of water and ice to reduce the temperature rise caused by these high speeds and viscosity of the mixture. A degassing process was also performed in a vacuum oven at room temperature for one hour in order to extract air bubbles produced through the mixing process. The hardener was then added and manually mixed with the modified resin using the ratio of 18 %wt of hardener in epoxy resin, according to the supplier data sheet (18% mix ratio by weight). The following relation was used to respect the final mass concentration of hardener within the epoxy.

$$M_h = 0.18 \cdot M_t \cdot \frac{1 - \%_{wt,g}}{1.18} \tag{3}$$

The nanocomposites plates (no fibers) were manufactured using the casting method. The mold was covered with a Polytetrafluoroethylene sheet (PTFE). Then, a sealing tape was added all around the mold and maintained using four pieces of wood strapped onto the mold with plastic hose clamp (Figure 2.1). In order to have a four millimeters thick plate, the plate surface was milled thereafter.

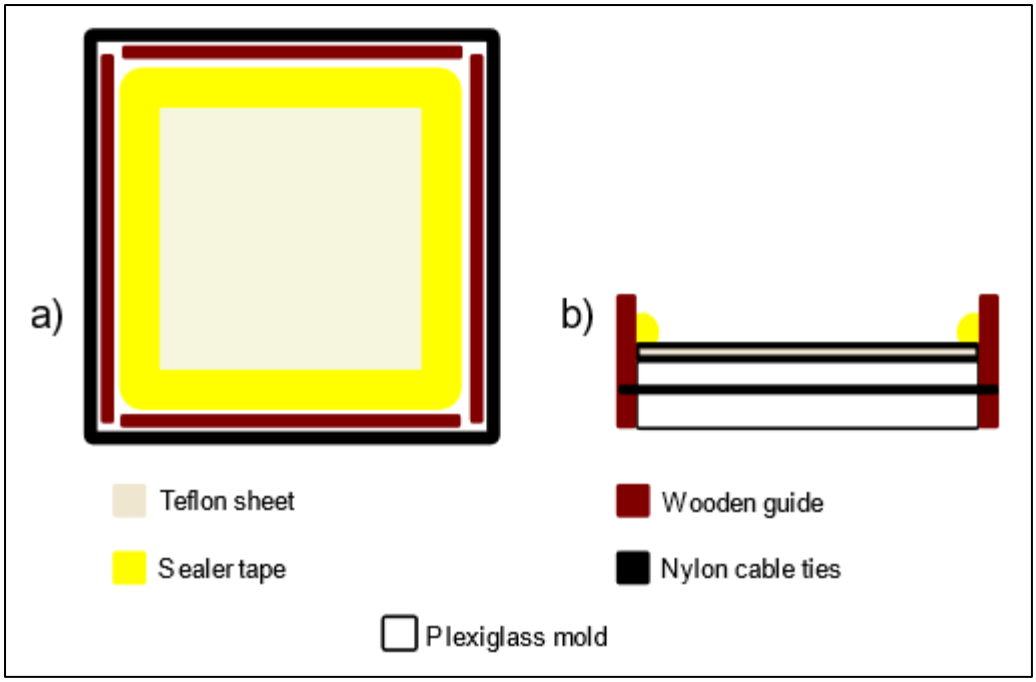

Figure 2.1 a) The casting mold used, b) Casting of 3%wt on the mold

The manufacturing process of CFRP laminates using viscous resin-graphene mixtures was challenging. Two major issues had to be addressed: ensuring a good and repeatable dispersion of graphene particles through the mixture as well as a constant and repeatable fiber volume fraction in all the laminates. The best process to address the graphene dispersion issue is the hand layup method. However, such an approach is prone to thickness variations, resulting in variations in the fiber volume fraction. Also, the resulting laminates are subject to porosity due to air trapped during the process. This is unacceptable to properly assess the graphene percentage effect on the machinability. Several methods have then been tested. First of all, the vacuum bagging approach was tested. The result did not live up to expectations, the upper side showed dry areas while the thickness variation from one laminate to the next was inconsistent. Next, the vacuum-assisted resin transfer molding approach (VARTM) was tested, but the result was not appropriate (Figure 2.3 a). The graphene was concentrated on a few top layers, which implies a non-homogeneous spatial distribution of the additive. The resin transfer molding (RTM, injection of the resin into a closed mold containing the reinforcement) was also tested. With this process, the graphene

distribution was good, but the top layers of fibers seemed to slip the ones on each other (Figure 2.3 b). These two manufacturing processes were not satisfactory in terms of repeatability and distribution of graphene to properly conduct this study.

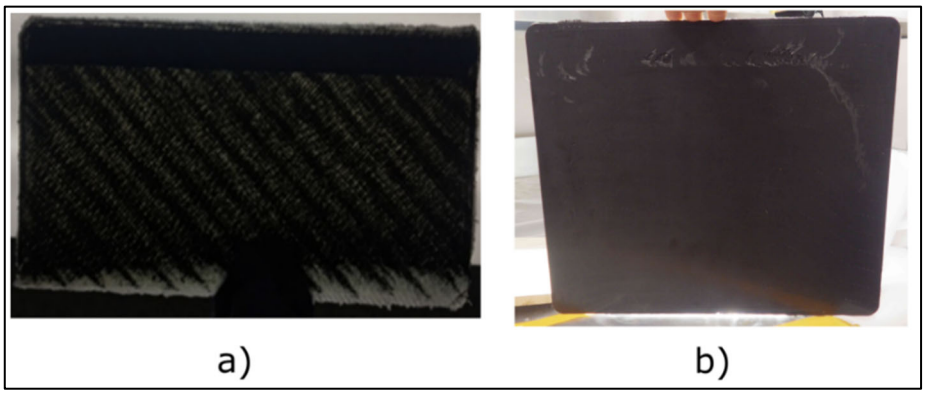

Figure 2.2 Glass fiber reinforced plastic with graphene a) VARTM method, b) RTM method

Following different iterations to fine-tune an adequate manufacturing process ensuring the proper distribution of the graphene with barely no porosity and consistent fiber volume fraction for all laminates, the combination of the lay-up process with vacuum bagging was found successful. In fact, the developed approach consists of a lay-up with vacuum bagging set up put under pressure using a hydraulic press at 1.5 MPa for three hours. In order to ensure an even thickness of the laminates, spacers were located at each corner of the mold, as shown in Figure 2.3. The breather was absent over the plate (as opposed to common approach) and placed only on the edge of the mold to absorb the excess of resin under the vacuum and pressure applied to the fibers layup. Sheets of polytetrafluoroethylene (PTFE) were also introduced between the composite as well as between the composite and the vacuum bag for an easier demolding of the plates. Furthermore, the resin cured was accelerated by heating the press plates at 66°C for three hours (Figure 2.3) as recommended in the epoxy resin manufacturer datasheet. Finally, to maximize curing, a post-curing step was realized using an oven (Despatch Thermal processing technology). The temperature was programed to respect an accurate curing cycle composed of three segments: ramp up rate at 10°C per hour until 66°C, steady temperature at 66°C for six hours and finally ramp

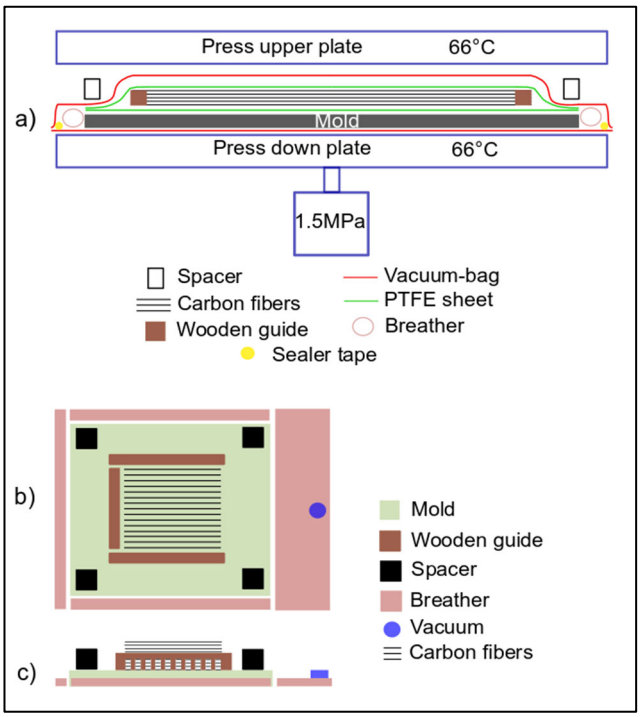

Figure 2.3 Set up of CFRP manufacturing: (a) front view, (b) upper view, (c) side view

down rate at 10°C per hour to reach room temperature. This last manufacturing process enables to have far less thickness variation, with precision to the tenth of a millimeter (Figure 2.4).

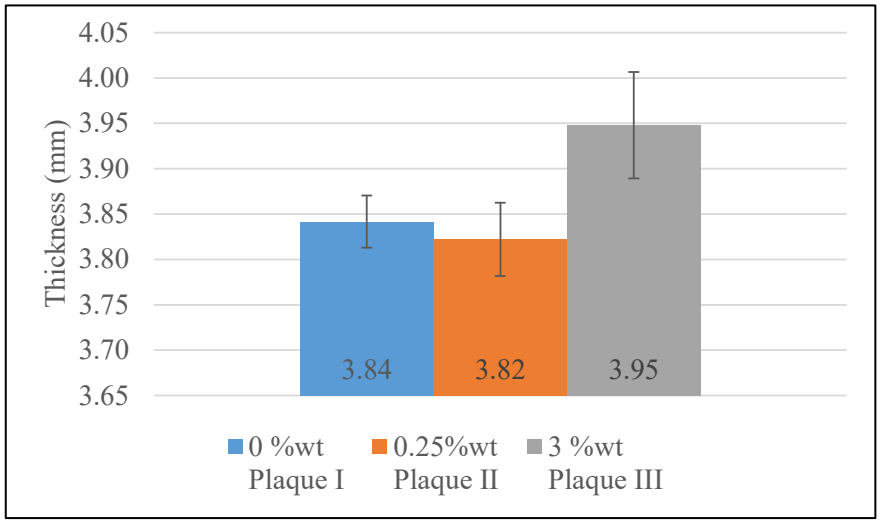

Figure 2.4 Thickness average of CFRP

2.2 Constituent content and porosity tests

The fiber volume fraction determines the mechanical and physical performance of FRP. The void fraction in turn reflects the quality of the piece and is of paramount importance on the final performance [24]. Two methods were used to measure the fiber and void contents. Firstly, the fiber volume fraction is determined with a method taking advantage of the thickness (which is quite constant). Then secondly, machine learning was used for the void fraction. The type of machine learning algorithms used depends on the chosen software. The machine learning software used for this study is ImageJ (National Institutes of Health) [25]. This method works well with carbon reinforcement [26]. Calculation of the void fraction using image processing of laminates taken under an optical microscope is found to be accurate and easy to implement [27]. A 50x magnification makes it possible to sufficiently highlight the voids [25,26,27].

Thus, with the thickness of the laminates, the fiber volume fraction is given by the equation:

$$v_f = \frac{N \cdot m_f}{\rho_f \cdot e} \tag{4}$$

With,

m_f the surface density of the fiber reinforcement ($g.m^{-2}$); ρ_f the specific gravity of the fibers ($kg.m^{-3}$); e the thickness of the laminates (m); N the number of plies of the laminates (Ø)

For this method, the fiber volume fractions were calculated for all CFRP laminates using equation 4 referring to the coupons thickness, measured after the plates machining. As shown in Figure 2.4, the thickness of the 0 %wt and 0.25 %wt plates are barely the same (20 µm). The maximum deviation observed is 110 µm (difference between the 0.25 %wt and the 3 %wt coupons). The 3 %wt plate is the thickest and this may be due to its resin, with higher viscosity, which is more difficult to drain and absorb by the breather. All the thicknesses are less than the shims thickness used in the manufacturing process (four

millimeters) because the vacuum bag has a variable thickness and decreases in thickness under the pressure of the hydraulic press over the shims.

All laminates manufactured were composed of 14 layers of carbon fibers at 90° ($[90_{14}]$) with respect to the feed direction of the cutting tool since this scheme represents the worst condition in terms of cutting forces and temperatures [5,21]. The surface density of unidirectional carbon fiber fabric used is $320\ g.m^{-2}$. The final target thickness of all laminates was four millimeters, which is representative of aerospace applications.

Another method and which is complementary to the first detailed above is to use the machine leaning to determine reliable void fractions [25,26]. Thus, the open-source software ImageJ™ (National Institutes of Health) [25] with the plug-in Weka Trainable using Image segmentation algorithm was used to calculate the void fraction [29]. This image processing aims to bring pixels together according to pre-defined criteria. Six edges samples per CFRP laminates were prepared to be polished by an automatic polisher (motopol 2000). Pictures were then taken using an optical microscope in order to have the whole edge area with a magnification of 50x (Figure 2.5 a). Finally, through the machine-learning software, two classes were created: voids and composite. Voids appear in red spots whereas the composite is in green in Figure 2.5 b. A last manipulation turns into black and white (Figure 2.5 c). Finally, the ratio of white to black pixels is calculated to obtain the void fraction.

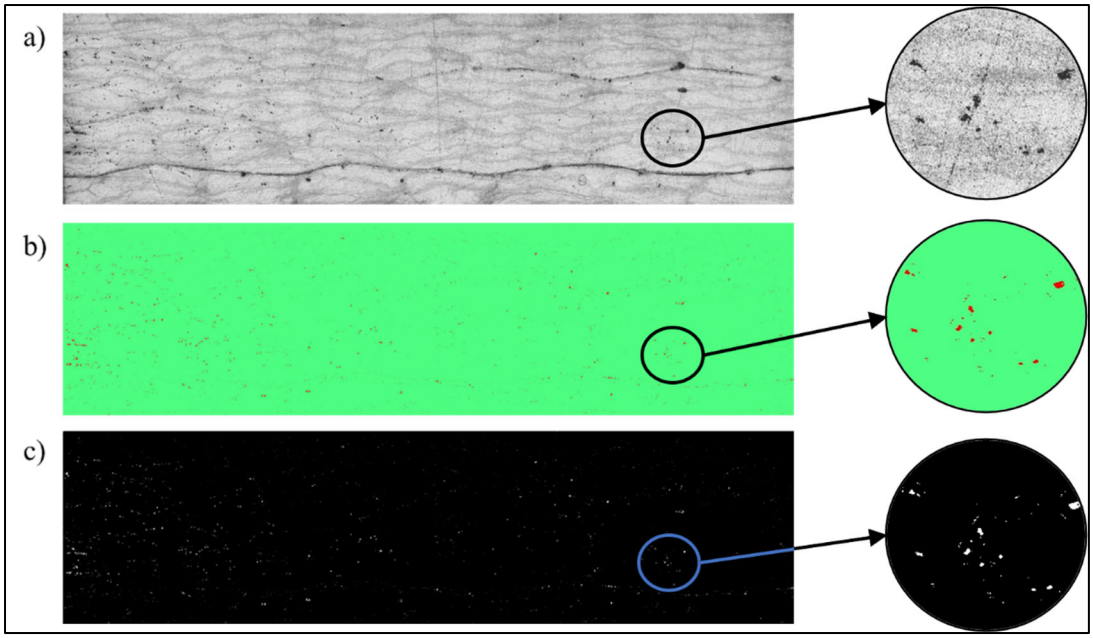

Figure 2.5 A sample of plate III (3%wt) a) microscope image, b) result of the machine learning, c) Black and white image for void calculation

2.3 Machining tests

The laminates were machined using a Huron K2X10 three-axis CNC machine in dry cutting conditions. The set-up uses a Kistler 9255B three-axis dynamometer for force measurement and acoustic emission for vibration monitoring. For temperature, a wireless system integrated to the tool holder (M320 Michigan Scientific) was used to record the cutting temperature. Two thermocouples type-K from Omega were bonded at the same height in each tooth of the PCD tool used. To guarantee a good accuracy of the recorded temperature, a very high thermal conductive cement (Omegabond 400) was used to create a thermal link between the tool and thermocouples while an epoxy glue was utilized to prevent any tearing during machining. An infrared camera (Grayess IRT Analyzer) was also used to complete the temperature reading (Figure 2.6 a).

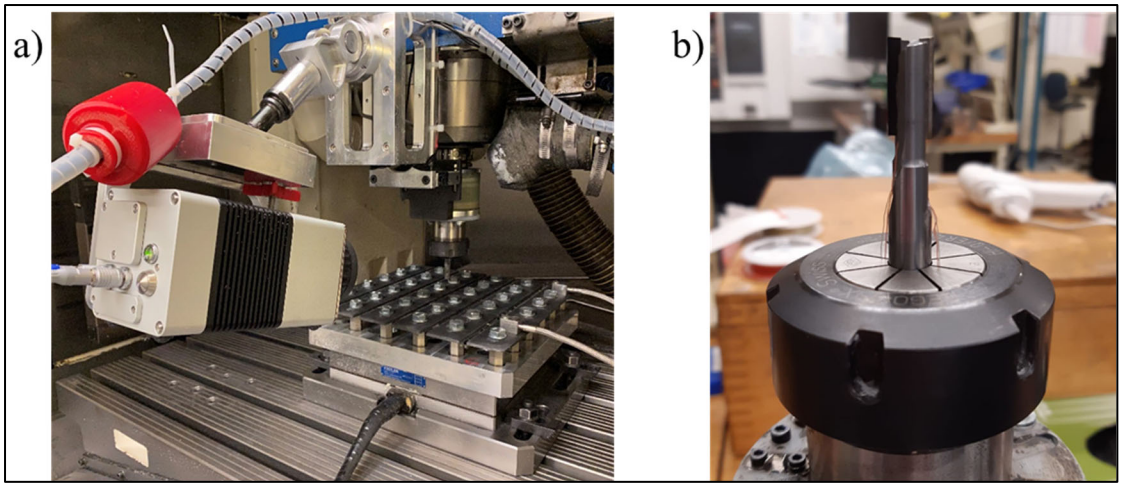

Figure 2.6 a) All the equipment of measurement in the CNC, b) Equipped PCD tool in tool holder

A PCD tool was selected for the machining tests for its excellent performance in previous studies [29,4,30] . Its characteristics are shown in Table 3. The cutting tool cuts the plate one after the other using a different cutting area (CA). As shown in Figure 2.7, the first cutting area (CA1) machine the CFRP plate while the second (CA2) machine the nanocomposite plate. We expect zero tool wear related to the nanocomposite specimens (CA2) due to their none abrasive nature and low mechanical strength [32].

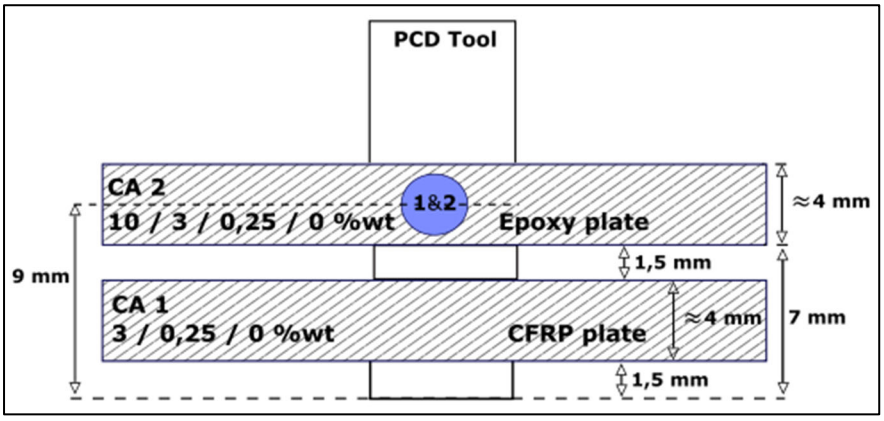

Figure 2.7 Cutting tool configuration

Taking into account the characteristics of the CNC and the PCD tool used as well as the optimal parameters found in the literature (cutting tool life and best quality of cut), the feed rate was set at 0.254 $mm.rev^{-1}$ and the cutting speed at 356 $m.min^{-1}$ [31].

Table 3 Cutting tool specification

Material	Diameter	Number of teeth	Edge radius	Rake angle	Clearance angle	Helix angle
Polycrystalline diamond (PCD)	0.95 mm	2	20 µm	10°	10°	0°

The CFRP and nanocomposite plates were machined using the slotting mode. As shown in Figure 2.8, each plate undergoes five machining passes which start on the same edge. This machining sequence involves that the tool between each pass exit the plate completely for a brief period to re-engage the tool in order to process the next pass. This configuration allows the thermal camera to always focus on a clear-cutting area (Figure 2.8).

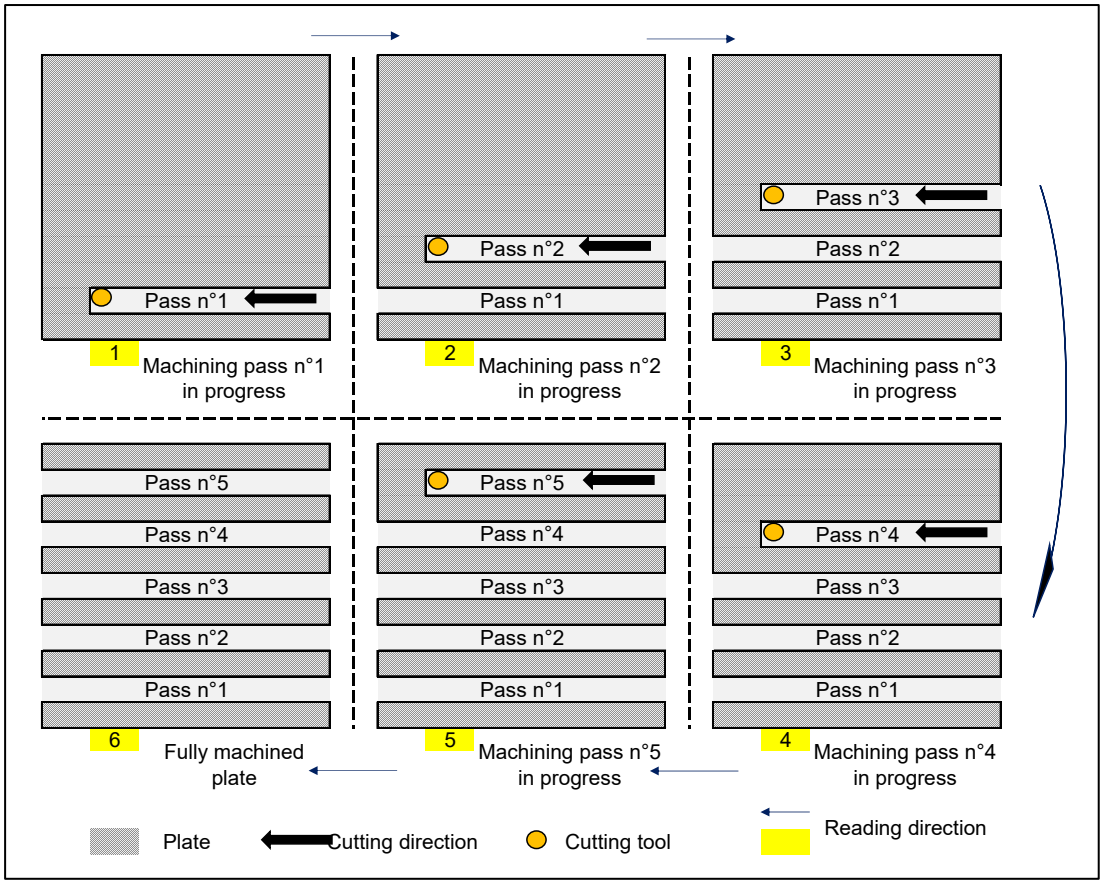

Figure 2.8 Machining sequence

As previously mentioned, the dimension of the machined plates were 30 x 30 cm. With the machining sequence described above, the total cutting distance is then 1.5 meters. With the cutting parameters (feed rate: 0.254 $mm.rev^{-1}$, cutting speed: 356 $m.min^{-1}$), the total machining time of each plate was 30 seconds.

2.4 Roughness measurement

Roughness measurements were recorded by a Mitutoyo SJ-410 profilometer. Given that full slotting is performed, two machined surfaces are obtained, one in up milling mode and the other in down milling mode. However, the up milling mode is considered as the most

relevant to compare surface roughness [10,32]. Thus, all the roughness measurements have been done on up milling surfaces of test coupons. In order to have the most reliable roughness, all the measurements were measured in the middle of each trimming pass with the profilometer settings selected to the ISO 4284-1997 standard (Table 4).

Table 4 Profilometer settings (sensitivity in µm)

Parameter	Ra
Sampling length	2.5 mm
Cut-off	2.5 mm / 8 mm
Number of measures	8 / 3
Evaluation length	20 mm / 24 mm
Number of points	4000 / 4800

3 Results and discussion

3.1 Fiber volume fraction

The void rate calculated using the "machine learning" approach described above, results in a value below one percent for all plates, which is quite low (Figure 3.1 a). This supports the fact that the CFRP manufacturing method is appropriate and that the results regarding the graphene effects on the trimming process will be relevant in this study. It can be observed in the figure that the void rate decreases with the increase in graphene concentration (Figure 3.1 a), which may appear as counterintuitive due to the difference in viscosity affecting the manufacturing process. This fluctuation may be explained by the fact that this method analyzes only surfaces and not volumes. Therefore, the images have intrinsic errors due to their discrete nature [28]. Thus this method involves a little more uncertainty than other methods by matrix digestion for example, which explains this

decrease in the void fraction with the percentage of graphene. However, the orders of magnitude are correct as compared to literature [27,25].

Regarding the fiber volume fraction, the plates having a 3% wt concentration have a lower fiber content, which is consistent to the fact that their thickness is slightly higher than for the two other concentrations (Figure 3.1). The maximum difference observed in the fiber content is 1.5%, which remains reasonable for the analysis regarding the effect of graphene on machinability (Figure 3.1 b).

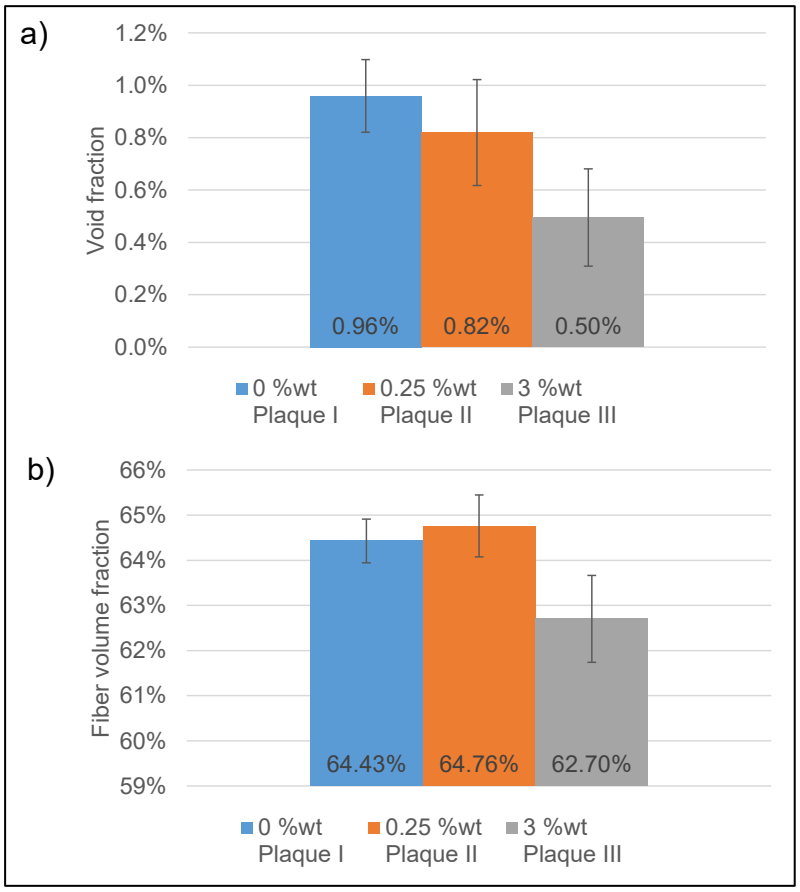

Figure 3.1 a) Void fraction, b) Fiber volume fraction

3.2 Cutting forces

Only the cutting forces of CFRP plates, measured by a dynamometric table (Kistler 9255B), were analyzed. Figure 3.2 shows the raw signal of the feed force for five passes of the cutting tool (Figure 2.8). As the tool used in this study generates very little axial force (zero helix angle), only the feed and normal forces were analyzed in this study.

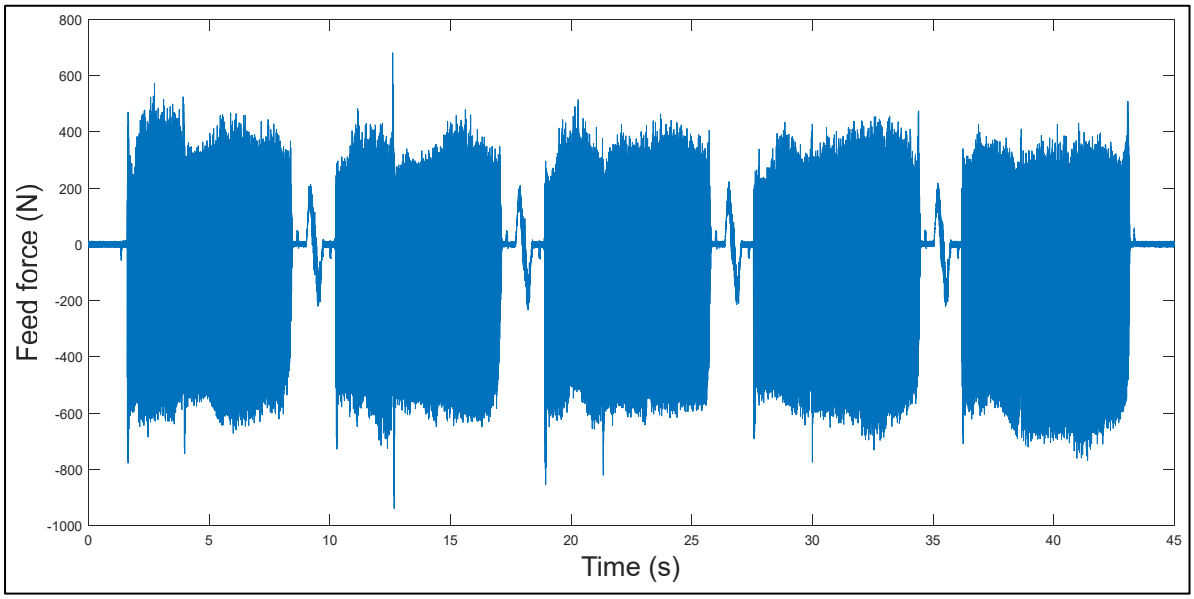

Figure 3.2 Raw feed force data, plate CFRP 0%wt

Figure 3.3 shows the feed and normal forces average. The average values were calculated considering 100 tool rotations in the middle of the signal for the five tool passes in order to avoid the noise generated when entering and leaving the plate by the cutting tool. A significant decrease in the feed force is observed when increasing the graphene concentration. The 3 %wt concentration reduced the cutting forces by 39.7% compared to 0 %wt. In contrast, the opposite is observed on the normal force (84.3%), i.e., the normal force increases with graphene concentration, nonetheless the recorded values remain very low. The trends are therefore opposite. In addition, the normal force is low compared to the feed force. Graphene therefore plays an important role in reducing the cutting forces (Figure 3.3).

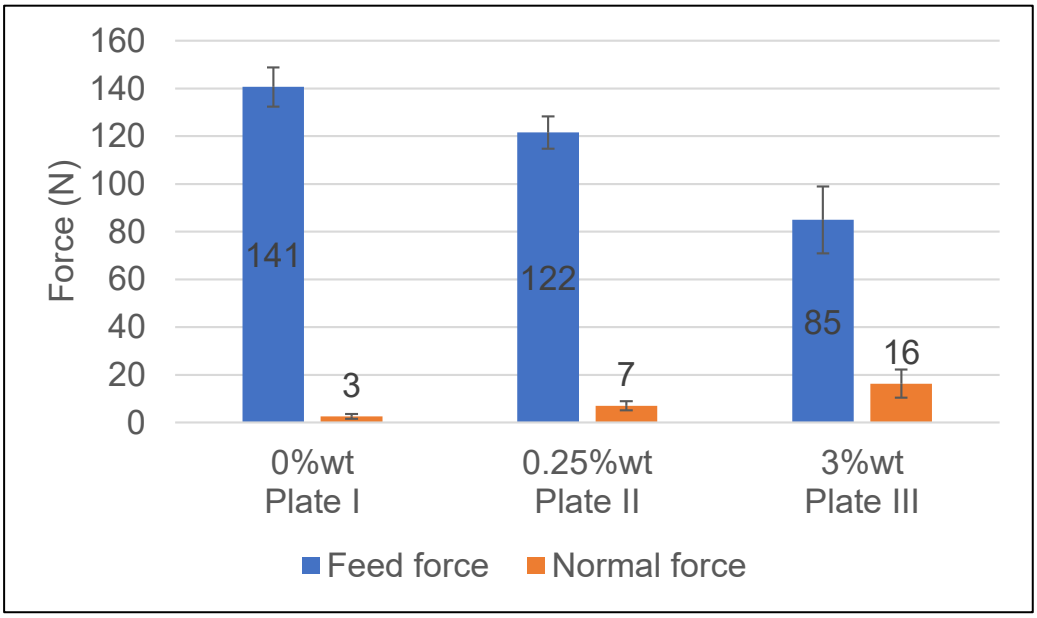

Figure 3.3 Cutting forces of CFRP plates

3.3 Cutting temperatures

Two temperature zones were studied, the first on the cutting tool during machining and the second on the machined material at the cut location. Two devices enabled the temperature readings, one corresponds to the thermocouples attached to the PCD cutting tool, the other one corresponds to the infrared camera. The thermocouples record the temperature on the tool while the thermal camera also measures the temperature of the tool (black square of 4 mm^2 in Figure 3.4) as well as the temperature of the material being machined (red rectangle of 2 mm^2, in Figure 3.4). The emissivity of the tool, as well as ones for the CFRP and epoxy plates were measured beforehand in order to calibrate the measurements of the thermal camera.

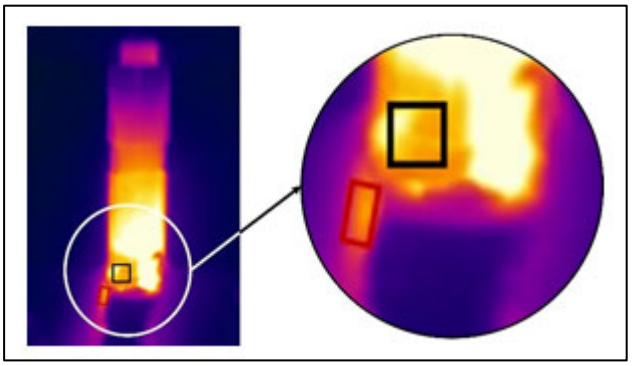

Figure 3.4 Thermal camera view, red rectangle (2 mm^2): cutting area, black square (4 mm^2): thermocouple area

In Figure 3.5 and Figure 3.6, the temperatures posted for a given graphene concentration are the average of the highest temperatures observed during a machining sequence, so five passes (1.5 meters of cutting length for 30 seconds of machining, Figure 2.8).

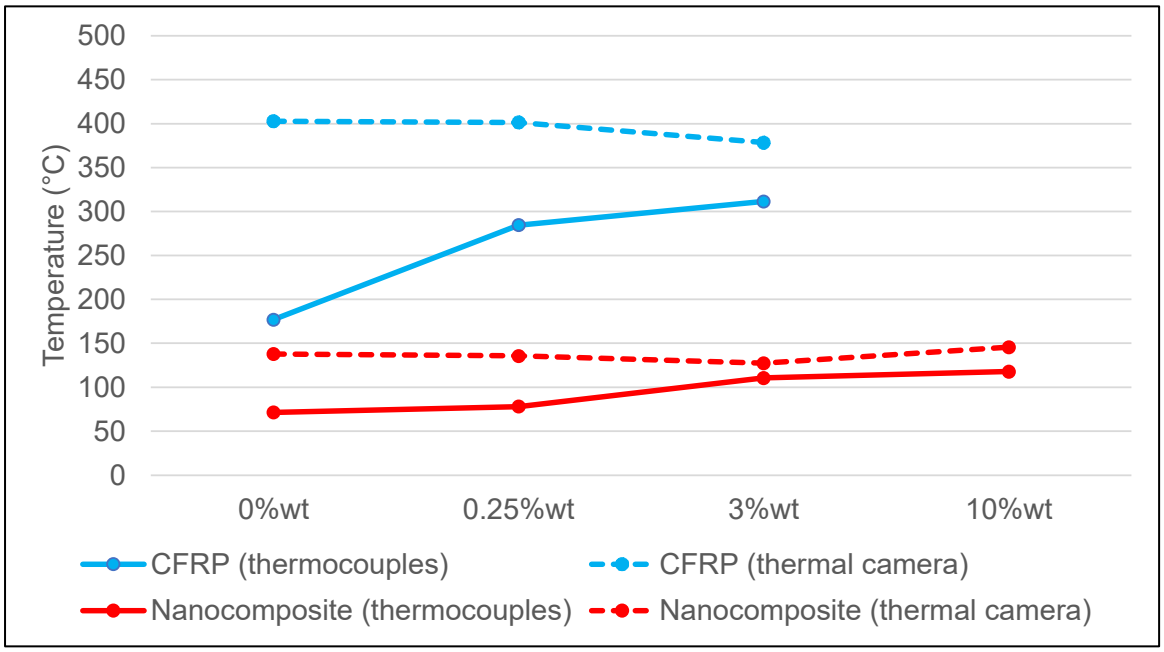

Figure 3.5 Tool temperature (thermocouples and thermal camera)

The temperature and trends obtained by the thermocouples and the thermal camera are different (Figure 3.5). They are much higher with the thermal camera. This difference can be explained by the thermocouples being glued to the tool by hand. Despite the thermal cement used ensures very good conduction, it takes longer for the heat to reach the tip of the thermocouple by conduction than what is required by the infrared radiation with the camera. The temperature recorded with the thermal camera was measured on the metal part of the tool, which is materialized by the black square in Figure 3.4. Indeed, the cutting tool used has a very high reflective part, the PCD blade, which acts like a mirror. Thermocouples measure temperature with a delay due to thermal inertia generated by the cutting tool, whereas the thermal camera which can directly measure the temperature by radiation, hence the significant difference in temperature observed between the two methods.

Regarding the results related to the thermocouples, the temperature of the tool increases with the graphene concentration for both the CFRP and modified epoxy plates (Figure 3.5). During CFRP machining, the temperature rises up to 200 °C for the plate with 0 %wt of graphene and up to 350 °C with a 3 %wt content of graphene. For the nanocomposite plates, the temperature rise is lesser, but ones can notice that it almost doubles between the 0 %wt and the 10%wt content of graphene. On the other hand, regarding the results related to the thermal camera, the trends are different. For the nanocomposites, the temperature recorded remains almost the same whatever their graphene content. For the CFRP plates, there is a significant drop in temperature for the highest graphene concentration (3%wt).

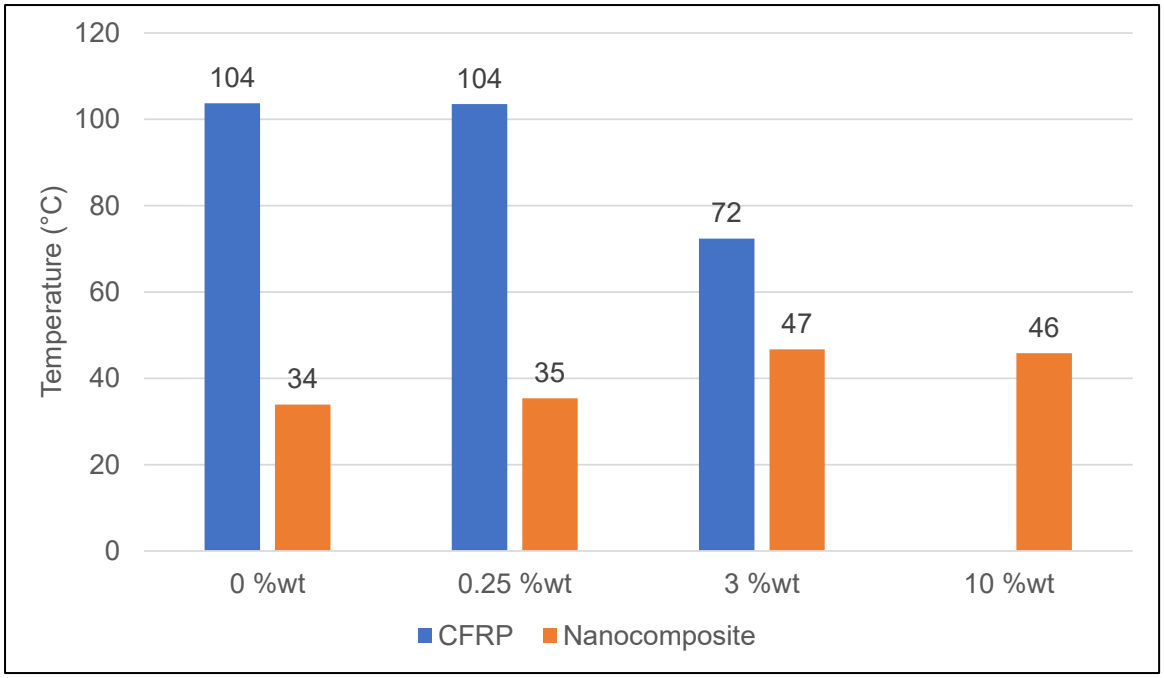

Figure 3.6 Cutting area temperature (thermal camera)

Observations made on the cutting area (black square in Figure 3.4) show that CFRP and nanocomposite plates have opposite temperature trends (Figure 3.6). For CFRP the temperature is around 100 °C for 0 and 0.25 %wt concentrations. The lowest temperature of 72 °C is obtained with the highest concentration, 3% wt. This represents a temperature decrease of almost 30%. So, in presence of graphene, the temperature of the machined CFRP plate decreases with an increase of graphene. When it comes to nanocomposite plates, the two lowest concentrations 0 and 0.25 %wt have similar temperatures near 35°C, while concentrations of 3 %wt and 10 %wt reach around 46°C, for a difference of only 11°C (Figure 3.6). Although graphene improves the thermal and mechanical properties of nanocomposites [19], it also brings a non-negligible gain in tenacity [34]. So, these two points, as advantages, largely outweigh the increase in temperature due to the thermal aspect.

3.4 Tool wear

As observed, no tool wear was noticed in the first cutting area (CA1, Figure 2.7) following the machining of all plates made with modified epoxy (0%wt – 10%wt) only. Concerning the second cutting area (CA2, Figure 2.7), the PCD tool did not undergo abnormal wear during the machining of the CFRP as attested by the rake and flank faces magnification shown in Figure 3.7. After machining the three CFRP plates, which represent a cutting length of 1.5 meter, the flank wear V_b [35,36] of the two flutes was measured and found to be respectively 50 and 51 micrometers (located between the two arrows, Figure 3.7 b). This tool wear on the flank face is uniform and has a much lower value than the commonly used criteria related to the end of tool life which is $V_b = 300$ micrometers.

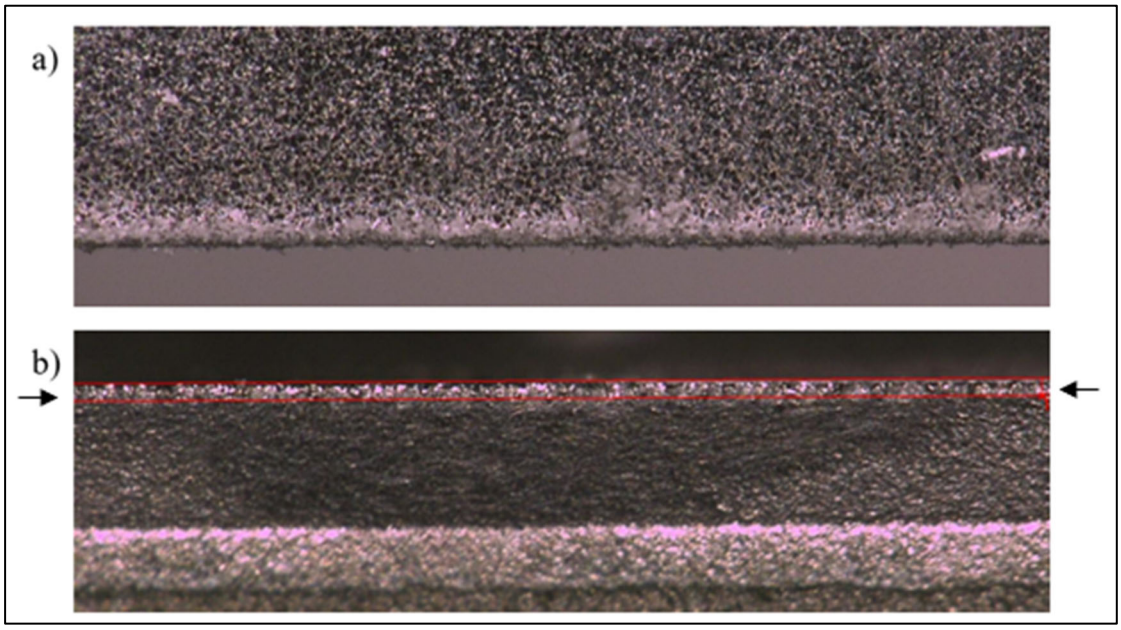

Figure 3.7 PCD Tool wear magnification 100 x, a) rake face, b) flank face

3.5 Roughness

The roughness was only measured on the CFRP in order to study the impact of graphene on it. The roughness R_a was measured on the edge in the middle of the CFRP plate, as

described in section 2.4. It tends to increase with the length of cut, based on a 1.5-meter length study. However, no matrix burning was noticed on all of the machined surfaces, which implies that no thermal damage has been induced to the resin. In addition, we must keep in mind that graphene in this study is not functionalized. Such an operation will allow better dispersion as well as a better affinity between graphene and epoxy, which would improve local thermal dissipation.

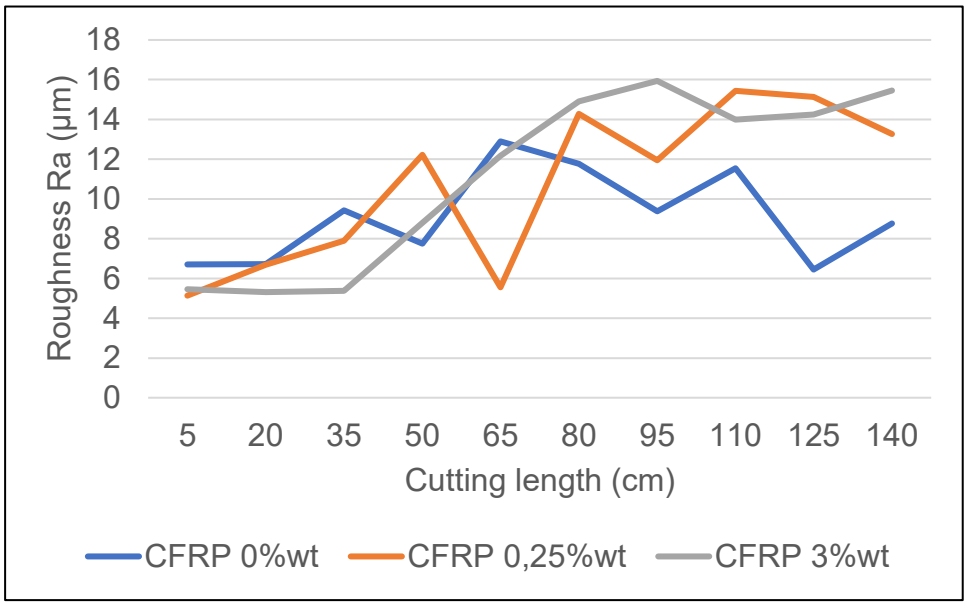

Figure 3.8 Roughness evolution

---

4 Conclusion

This study demonstrates the influence of graphene during machining. Two types of materials were manufactured and tested, CFRP laminates and modified resin plates (nanocomposites), with graphene concentrations ranging from 0 to 10% wt. The manufacturing process of all the laminates provided excellent repeatability in terms of quality, fiber volume fraction and void fraction, allowing the study of graphene on

machinability to be relevant. The machining set up utilized for the experiments allowed force measurement and temperature measurement using infrared camera as well as thermocouples fixed to the cutting tool. This study confirmed that graphene addition to epoxy has a significant influence on cutting temperature and cutting forces. The main contributions of graphene on the machinability of both materials are:

- The feed forces decrease significantly while trimming CFRP, up to 43% with 0.25 %wt of graphene. The highest concentration (3 %wt) lead to the lowest feed forces.
- The temperature has different influence depending on the measurement method (thermocouples, thermal camera) and the location (cutting aera, thermocouples aera). The temperatures recorded on thermocouples aera with CFRP composites, temperatures increase with the percentage of graphene (thermocouples method). The opposite is observed with the thermal camera. On the other hand, the temperatures increase whether with the thermal camera or thermocouples. However, in the cutting area (in the flute of the tool), the trends between CFRPs and nanocomposites are opposite. The temperature decreases with the amount of graphene for the CFRP (15% reduction in temperature with 3% wt) whereas for nanocomposite the temperature increases slightly with the concentration of graphene.

Improvements can be made by using a more suitable resin and by functionalizing graphene in order to improve the dispersion, avoid agglomerations of graphene and therefore decrease the abrasiveness.

Another improvement could be to manufacture prepregs impregnated with graphene. This could control the distribution of graphene and avoid homogenization problem during the manufacture of FRP. With the manufacturing method proposed in this study, a higher pressure is required to increase the accuracy of the final thickness.

Machine learning void rate evaluation is a promising non-destructive method. The magnification x100 could be interesting to refine void rate measurement. The use of a confocal microscope for the would be interesting alternative method to be a non-destructive

analysis of the surface roughness measurements.

The development of an energy balance associated with a numerical model of heat dissipation will improve understanding of the role of graphene in machining and anticipate tool wear and surface roughness. At the same time, to characterize the tool wear as well as the associated roughness, a machining with a long cut can be very interesting.

Statements & Declarations

a. **Funding** This research was funded by National Research Council of Canada (NSERC grant NSERC EGP534389-18) and NanoXplore inc.

b. **Conflicts of interest** The authors state that they have no known competing financial interests or personal relationships that could have influenced the research presented in this study.

c. **Availability of data and material** Not applicable.

d. **Code availability** Not applicable.

e. **Ethics approval** The authors confirm to the work's novelty and state that it has not been submitted to any other journal.

f. **Consent to participate** The authors give consent to participate.

g. **Consent for publication** The authors give their consent for their work to be published.

References

[1] M. Ashby, H. Shercliff, and D. Cebon, *Matériaux: Ingénierie, science, procédé et conception*. Presses polytechniques et universitaires romandes, 2013. [Online]. Available: https://books.google.ca/books?id=eGUGDQAAQBAJ

[2] M. Mrazova, 'Advanced composite materials of the future in aerospace industry', *INCAS Bull.*, vol. 5, no. 3, pp. 139–150, Sep. 2013, doi: 10.13111/2066-8201.2013.5.3.14.

[3] M. Altin Karataş and H. Gökkaya, ‘A review on machinability of carbon fiber reinforced polymer (CFRP) and glass fiber reinforced polymer (GFRP) composite materials’, *Def. Technol.*, vol. 14, no. 4, pp. 318–326, Aug. 2018, doi: 10.1016/j.dt.2018.02.001.

[4] R. Komanduri, ‘Machining of fiber-reinforced composites’, *Mach. Sci. Technol.*, vol. 1, no. 1, pp. 113–152, Aug. 1997, doi: 10.1080/10940349708945641.

[5] Jahanmir, *Machining of Ceramics and Composites*. CRC Press, 1999.

[6] R. Teti, ‘Machining of Composite Materials’, vol. 51, p. 24, 2002.

[7] J. Turner, R. J. Scaife, and H. M. El-Dessouky, ‘Effect of machining coolant on integrity of CFRP composites’, *Adv. Manuf. Polym. Compos. Sci.*, vol. 1, no. 1, pp. 54–60, Feb. 2015, doi: 10.1179/2055035914Y.0000000008.

[8] D. Iliescu, ‘Approches experimentale et numerique de l’usinage a sec des composites carbone/epoxy’, 2008. [Online]. Available: https://pastel.archives-ouvertes.fr/pastel-00005136

[9] H. Hamedanianpour and J. F. Chatelain, ‘Effect of Tool Wear on Quality of Carbon Fiber Reinforced Polymer Laminate during Edge Trimming’, *Appl. Mech. Mater.*, vol. 325–326, pp. 34–39, Jun. 2013, doi: 10.4028/www.scientific.net/AMM.325-326.34.

[10] J. Delahaigue, J.-F. Chatelain, and G. Lebrun, ‘Influence of Cutting Temperature on the Tensile Strength of a Carbon Fiber-Reinforced Polymer’, *Fibers*, vol. 5, no. 4, p. 46, Dec. 2017, doi: 10.3390/fib5040046.

[11] G. Mullier and J. F. Chatelain, ‘Influence of Thermal Damage on the Mechanical Strength of Trimmed CFRP’, vol. 9, no. 8, p. 8, 2015.

[12] V. Lopresto, A. Caggiano, and R. Teti, ‘High Performance Cutting of Fibre Reinforced Plastic Composite Materials’, *Procedia CIRP*, vol. 46, pp. 71–82, 2016, doi: https://doi.org/10.1016/j.procir.2016.05.079.

[13] K.-M. Li, C. Wang, and W.-Y. Chu, ‘An improved remote sensing technique for estimating tool–chip interface temperatures in turning’, *J. Mater. Process. Technol.*, vol. 213, no. 10, pp. 1772–1781, Oct. 2013, doi: 10.1016/j.jmatprotec.2013.04.014.

[14] E. P. Randviir, D. A. C. Brownson, and C. E. Banks, ‘A decade of graphene research: production, applications and outlook’, *Mater. Today*, vol. 17, no. 9, pp. 426–432, 2014, doi: https://doi.org/10.1016/j.mattod.2014.06.001.

[15] Jiacheng Wei, Mohd Saharudin, Thuc Vo, and Fawad Inam, ‘N,N-Dimethylformamide (DMF) Usage in Epoxy/Graphene Nanocomposites: Problems Associated with Reaggregation’, *Polymers*, vol. 9, no. 12, p. 193, May 2017, doi: 10.3390/polym9060193.

[16] K. Al Imran, ‘Enhancement of electrical conductivity of carbon/epoxy composites by graphene and assessment of thermal and mechanical properties’, 2016.

[17] D. Zhang, L. Ye, S. Deng, J. Zhang, Y. Tang, and Y. Chen, ‘CF/EP composite laminates with carbon black and copper chloride for improved electrical conductivity and interlaminar fracture toughness’, *Compos. Sci. Technol.*, vol. 72, no. 3, pp. 412–420, Feb. 2012, doi: 10.1016/j.compscitech.2011.12.002.

[18] M. Wang, C. Yan, and L. Ma, ‘Graphene Nanocomposites’, in *Composites and Their Properties*, N. Hu, Ed. Rijeka: IntechOpen, 2012. doi: 10.5772/50840.

[19] H. Lentzakis *et al.*, ‘Mechanical, Thermal and Electrical Property Enhancement of Graphene-Polymer Nanocomposites’, p. 5, 2017.

[20] J. Keyte, K. Pancholi, and J. Njuguna, ‘Recent Developments in Graphene Oxide/Epoxy Carbon Fiber-Reinforced Composites’, *Front. Mater.*, vol. 6, p. 224, 2019, doi: 10.3389/fmats.2019.00224.

[21] K. El-Ghaoui, J.-F. Chatelain, and C. Ouellet-Plamondon, ‘Effect of Graphene on Machinability of Glass Fiber Reinforced Polymer (GFRP)’, *J. Manuf. Mater. Process.*, vol. 3, no. 3, p. 78, Sep. 2019, doi: 10.3390/jmmp3030078.

[22] S. Ghafarizadeh, G. Lebrun, and J.-F. Chatelain, ‘Experimental investigation of the cutting temperature and surface quality during milling of unidirectional carbon fiber reinforced plastic’, *J. Compos. Mater.*, vol. 50, no. 8, pp. 1059–1071, Apr. 2016, doi: 10.1177/0021998315587131.

[23] M. Ali Charfi, R. Mathieu, J.-F. Chatelain, C. Ouellet-Plamondon, and G. Lebrun, ‘Effect of Graphene Additive on Flexural and Interlaminar Shear Strength Properties of Carbon Fiber-Reinforced Polymer Composite’, *J. Compos. Sci.*, vol. 4, no. 4, p. 162, Oct. 2020, doi: 10.3390/jcs4040162.

[24] D. Saenz-Castillo, M. I. Martín, S. Calvo, F. Rodriguez-Lence, and A. Güemes, ‘Effect of processing parameters and void content on mechanical properties and NDI of thermoplastic composites’, *Compos. Part Appl. Sci. Manuf.*, vol. 121, pp. 308–320, Jun. 2019, doi: 10.1016/j.compositesa.2019.03.035.

[25] C. Schneider, W. Rasband, and K. Eliceiri, ‘NIH Image to ImageJ: 25 years of image analysis’, *Nat. Methods*, vol. 9, Jul. 2012, doi: 10.1038/nmeth.2089.

[26] A. H. Kite, D. K. Hsu, D. J. Barnard, D. O. Thompson, and D. E. Chimenti, ‘Determination of porosity content in composites by micrograph image processing’, in *AIP Conference Proceedings*, Golden (Colorado), 2008, vol. 975, pp. 942–949. doi: 10.1063/1.2902767.

[27] C. Santulli, R. G. Gil, A. C. Long, and M. J. Clifford, ‘Void Content Measurements in Commingled E-Glass/ Polypropylene Composites Using Image Analysis from Optical Micrographs’, *Sci. Eng. Compos. Mater.*, vol. 10, no. 2, Jan. 2002, doi: 10.1515/SECM.2002.10.2.77.

[28] L. Di Landro, A. Montalto, P. Bettini, S. Guerra, F. Montagnoli, and M. Rigamonti, ‘Detection of Voids in Carbon/Epoxy Laminates and Their Influence on Mechanical Properties’, *Polym. Polym. Compos.*, vol. 25, no. 5, pp. 371–380, Jun. 2017, doi: 10.1177/096739111702500506.

[29] I. Arganda-Carreras, *Trainable Weka Segmentation: a machine learning tool for microscopy pixel classification.*, vol. 33, no. 15. Oxford Univ Press, 2017. doi: 10.1093/bioinformatics/btx180.

[30] M. H. El-Hofy, S. L. Soo, D. K. Aspinwall, W. M. Sim, D. Pearson, and P. Harden, ‘Factors Affecting Workpiece Surface Integrity in Slotting of CFRP’, *Procedia Eng.*, vol. 19, pp. 94–99, 2011, doi: 10.1016/j.proeng.2011.11.085.

[31] S. Bérubé, ‘Usinage en détourage de laminés composites carbone/époxy’, Mémoire de maîtrise, École de technologie, 2014.

[32] J. W. Carr and C. Feger, ‘Ultraprecision machining of polymers’, *Precis. Eng.*, vol. 15, no. 4, pp. 221–237, 1993, doi: https://doi.org/10.1016/0141-6359(93)90105-J.

[33] W. König, C. Wulf, P. Graß, and H. Willerscheid, ‘Machining of Fibre Reinforced Plastics’, *CIRP Ann.*, vol. 34, no. 2, pp. 537–548, 1985, doi: https://doi.org/10.1016/S0007-8506(07)60186-3.

[34] R. Atif, I. Shyha, and F. Inam, ‘Mechanical, Thermal, and Electrical Properties of Graphene-Epoxy Nanocomposites—A Review’, *Polymers*, vol. 8, no. 8, p. 281, Aug. 2016, doi: 10.3390/polym8080281.

[35] G. Li, M. Z. Rahim, W. Pan, C. Wen, and S. Ding, 'The manufacturing and the application of polycrystalline diamond tools – A comprehensive review', *J. Manuf. Process.*, vol. 56, pp. 400–416, Aug. 2020, doi: 10.1016/j.jmapro.2020.05.010.

[36] L. Norberto López de Lacalle, F. J. Campa, and A. Lamikiz, '3 - Milling', in *Modern Machining Technology*, J. Paulo Davim, Ed. Woodhead Publishing, 2011, pp. 213–303. doi: 10.1533/9780857094940.213.